Proceedings of the ASME 2010 3rd Joint US-European Fluids Engineering Summer Meeting and 8th International Conference on Nanochannels, Microchannels, and Minichannels
FEDSM-ICNMM2010
August 1-5, 2010, Montreal, Canada

FEDSM-ICNMM2010-30647

NUMERICAL INVESTIGATION OF HEAT TRANSFER ENHANCEMENT IN A MICROCHANNEL WITH OFFSET MICRO PIN-FINS

Haleh Shafeie
School of Mechanical Engineering
Shiraz University
Shiraz, Iran

Omid Abouali
School of Mechanical Engineering
Shiraz University
Shiraz, Iran
abouali@shirazu.ac.ir

Khosrow Jafarpur
School of Mechanical Engineering
Shiraz University
Shiraz, Iran
kjafarme@shirazu.ac.ir

ABSTRACT

This paper presents a numerical study of laminar forced convection in microchannels network heat sinks with fabricated offset pin-fins. A 3-dimensional mathematical model, for conjugate heat transfer in both solid and liquid is presented. For this aim the Navier-Stokes and energy equations for the liquid region and the energy equation for the solid region are solved simultaneously and the pressure drop together heat transfer characteristics of a single-phase microchannel heat sink were investigated. A typical microchannel was selected and it was shown that using offset pin-fins has a noticeable effect and heat removal rate can be increased using this technique. However the pressure drop is also highly increasing which leads to a low coefficient of performance for microchannel with this type of micro-structure.

NOMENCLATURE

A_{ch}	cross-sectional of channel
A_{free}	free flow area
C_p	specific heat capacity
H	height of unit channel
H_{ch}	height of channel
H_{w1}	cover plate thickness
H_{w2}	thickness from the unit cell bottom to the channel bottom
K	thermal conductivity
L	length of unit cell
P	pressure
P	pressure drop
Re	Reynolds number
S	Distance between pin-fin rows
T	temperature
T_{in}	fluid inlet temperature
U_{in}	inlet velocity
$\boldsymbol{V}$	velocity vector
W_f	fin thickness ($W_f = 2W_w$)
W	width of unit cell
W_{ch}	channel width
W_w	half-width of the fin thickness
b	width of the substrate
f	friction factor
h_1	height of short pin-fins
h_2	height of tall pin-fins
n	number of pin-fins
q	heat flux
μ	dynamic viscosity
ρ	density

Sub-indexes

f	fluid
s	solid
in	inlet
out	outlet
fd	fully developed

INTRODUCTION

Over the past two decades, the need for the removal of a large amount of heat from a small area has led to too many researches in connection with the microchannel heat sinks (MCHS). The heat sink is usually made from a solid with high thermal conductivity such as silicon or copper. Microchannels are fabricated into the surface of this solid part by micro-fabrication technology. Microchannel heat sinks combine the

attributes of very high surface area to volume ratio, large convective heat transfer coefficient as well as small mass, volume and coolant inventory. These heat sinks are very suitable for cooling devices such as high performance microprocessors.

Rectangular geometries are of particular interest in micro-fluidics applications. Shah and London [1] and Kakac *et al.* [2] proposed comprehensive summaries of the available literature. Kishimoto and Sasaki [3] proposed the use of enhanced microchannels. Morini [4] reviewed the convective heat transfer through microchannels. The need for higher heat transfer coefficients than those attainable with plain microchannels was emphasized by Kandlikar and Grande [5] and some specific enhancement geometries were suggested by Steinke and Kandlikar [6, 7]. Kandlikar and Upadhye [8] analyzed enhanced offset strip-fins geometry. Colgan *et al.* [9] proposed detailed experimental results comparing various offset fin geometries. They plotted the curves of apparent friction factors and Nusselt numbers for plain and several enhanced configurations. Tao *et al.* [10] proposed three possible mechanisms for the single-phase heat transfer enhancement. These mechanisms are: (1) decreasing the thermal boundary layer; (2) increasing flow interruptions; and (3) increasing the velocity gradient near the heated surface. It is the manipulation of these three mechanisms that results in heat transfer augmentation. Croce *et al.* [11] simulated roughness as a set of three-dimensional conical peaks distributed on the ideal smooth surfaces of a plane microchannel. They investigated the effect of roughness on microchannel heat transfer and pressure drop. In a numerical simulation, Cheng [12] worked on a stacked two-layer microchannel heat sink with enhanced mixing passive microstructure. They found the stacked microchannel with passive structures has better performance than the smooth microchannels. Zhong *et al.* [13] tried to simulate a series of CNT (Carbon Nano-tube) micro-fin cooling architectures based on two dimensional fin array models. They studied the influence of micro-fin structures, flow velocity, heating powers and effective thermal conductivity on cooling effects. Hasan *et al.* [14] examined the effect of size and shape of microchannels on the thermal and hydraulic performance of a heat exchanger. Hong and Cheng [15] investigated laminar forced convection of water in offset strip-fin microchannels network heat sinks for microelectronic cooling. Kosar [16] studied the influence of substrate thickness and material on heat transfer in microchannel heat sinks.

In the present work, the flow field and heat transfer for a microchannel with special offset microstructure pin-fins are studied numerically and the heat transfer enhancement and the pressure drop due to cylindrical microstructures are investigated as well.

MODEL DESCRIPTION

A microchannels heat sink with 1 cm width and 2.09 cm length similar to numerical works of Kosar [16] and Abouali and Baghernezhad [17] was selected for numerical study in the present work. Eighteen channels were fixed in the given width. The channels were equidistantly spaced within the 1 cm heat sink width and had the cross-sectional dimensions of 500μm width and 90μm height.

In this paper we examine the use of structures formed in the bottom of the channel as shown in figure 1. The repeated microstructure pattern within the microchannel is a row of four cylinders inclined at 45° to the direction of the flow. The posts have a diameter of about 80 μm. It can be clearly seen that the rows alternate between tall posts with a height equal to the depth of the channel and shallow posts having a height of about 60 μm. Figure 2 shows a scanning electron micrograph of this type of micro-structures presented by Kandlikar and Grande [5]. In their work, this type of mircochannel was presented as a possible way to enhance the heat transfer. In the present work the heat transfer characteristic in a microchannel with these types of micro pin-fins has been investigated.

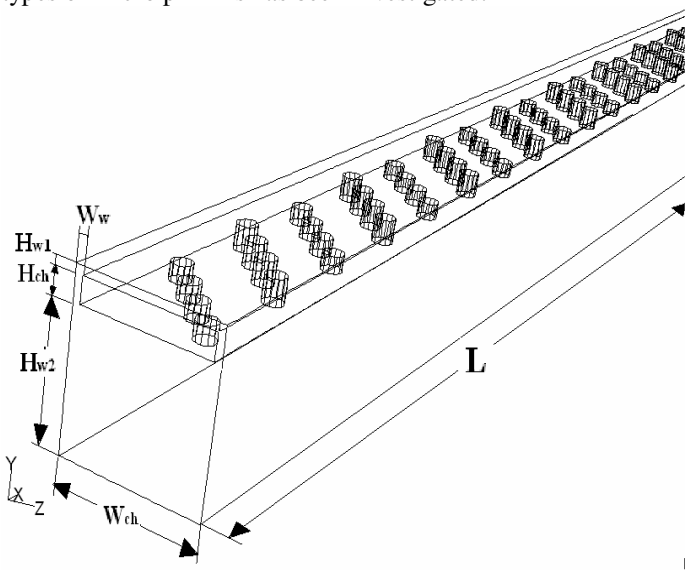

Figure 1. Schematic of the heat sink unit cell for the numerical simulation with structures formed in the bottom surface of the microchannel.

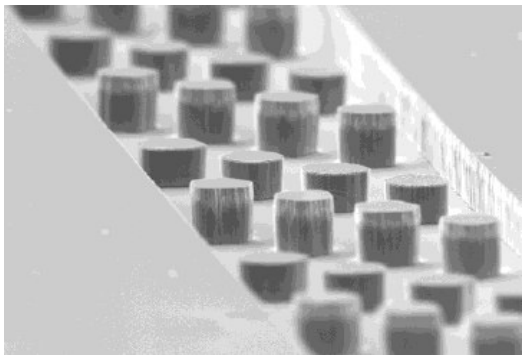

Figure 2. Scanning electron micrograph of posts within a microchannel. Successive rows of posts are alternately tall and shallow. Used by permission of Kandlikar and Grande [5].

A unit cell containing a single microchannel is chosen to perform the numerical analysis. Symmetry allows these results to be easily extended to the entire heat sink. Also Figure 1 illustrates the unit cell, the corresponding coordinate system and key notations. Dimensions of the unit cell are given in Table 1.

Table 1. Dimensions of the microchannel heat sink

W_{ch} (μm)	W_w (μm)	H_{ch} (μm)	H_{w1} (μm)	H_{w2} (μm)	L(cm)
500	27	90	30	500	2.09

Considering the geometry of the microchannel with water as the fluid, the following assumptions are made:
1. Flow is steady, laminar, and incompressible.
2. Radiation heat loss is negligible.
3. Properties except water viscosity are constant for fluid and solid materials.
4. Body force was neglected.

GOVERNING EQUATIONS

- Governing Equations for Fluid

Based on the above assumptions, the governing differential equations used to describe the fluid flow and heat transfer in the unit cell are as follows. For the cooling water, the continuity, momentum, and energy equations are expressed respectively as

$$\nabla \cdot V = 0 \quad (1)$$

$$\rho_f (V.\nabla V) = -\nabla P + \nabla(\mu_f \nabla V) \quad (2)$$

$$\rho_f C_p (V.\nabla T) = k_f \nabla^2 T \quad (3)$$

- Governing Equations for Solid

For the solid region, the energy equation is

$$k_s \nabla^2 T = 0 \quad (4)$$

- Boundary Conditions

For flow boundary conditions, a uniform velocity was applied at the channel inlet. This velocity is computed based on the Reynolds number of the flow. Moreover the flow is assumed fully developed at the channel outlet, and the velocity is zero along all other solid boundaries.

To set the thermal boundary conditions in the solid region, a constant temperature is applied at the unit cell bottom Ts= 85°C, and a constant temperature Tin was set at the inlet of the channel. Other surfaces are considered adiabatic or symmetric.

Numerical simulation is based on a finite volume formulation. An available computer code was used for numerical simulation in present work. The discretized governing equations were solved by employing SIMPLE algorithm for the pressure correction processes, and convective and diffusive terms are discretized by upwind and central difference schemes, respectively. In addition, the grid independent study was done, and a structured grid with total number of about 1,300,000 elements was selected for the numerical model with highest number of pin-fins.

RESULTS AND DISCUSSION

-Validation of the Numerical Model

The numerical model was validated before by Abouali and Baghernezhad [17]. The same procedure was done in present work and is not brought here for sake of brevity.

-Results

The effect of pin-fins is studied for different cases. Table 2 shows a brief description of these cases. The first case includes 50 equidistantly rows. The distance between the rows is 400μm and the first row starts with short cylinders. The heights of the cylinders change alternately between 90 and 60 μm. The second case includes 50 rows and all cylinders are tall (90 μm height). For the third case all cylinders in 50 rows are short (60 μm height). The forth case includes 25 rows with equally 800μm distance and the first row starts with short cylinder that height of cylinders change alternately. In the fifth and sixth cases all cylinders in 25 rows are tall and short respectively. The seventh case includes 13 rows with equally 1200μm distance and rows are alternately short and tall. In the eighth and ninth cases all cylinders in 13 rows are tall and short respectively. We compared these cases with a simple microchannel that has 500 μm width and all kinds of microchannels have equal mass flow rates.

Table 2. Number of micro-pins for various studied cases

	TYPES	NUMBER OF ROWS	NUMBER OF TALL PINS	NUMBER OF SHORT PINS	ROWS DISTANCES (μM)
1	**Short and Tall Fins (50 Rows)**	50	100	100	400
2	**All Fins Tall (50 Rows)**	50	200	0	400
3	**All Fins Short (50 Rows)**	50	0	200	400
4	**Short and Tall Fins (25 Rows)**	26	52	52	800
5	**All Fins Tall (25 Rows)**	26	104	0	800
6	**All Fins Short (25 Rows)**	26	0	104	800
7	**Short and Tall Fins (13 Rows)**	13	24	28	1200
8	**All Fins Tall (13 Rows)**	13	52	0	1200
9	**All Fins Short (13 Rows)**	13	0	52	1200

Figure 3 compares the maximum heat removal for pin-finned microchannels at constant substrate temperature and Re= 387 in all above cases and also a simple microchannel. As Figure 3 shows using pin-fins micro structures can enhance the heat removal flux from 206 w/cm^2 for the simple microchannel to 280 w/cm^2 for the case with 50 rows tall fins. Also the differences between heat removals of various heights of micro pin-fins are not significant. Also the difference for the layout of the fins i.e. starting either by tall or short fins does not have a noticeable effect on heat transfer (results not shown here).

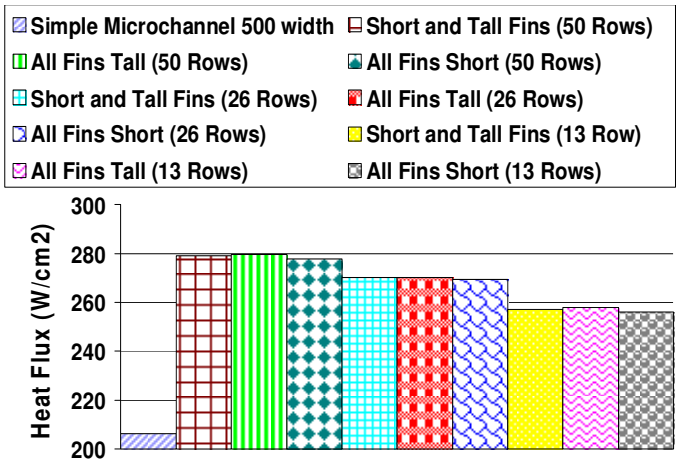

Figure 3 Comparison between microchannels with different schemes of pin-fins microstructure for maximum heat removal flux , T_s= 85° C, Re= 387.

The physical reason of this enhancement in heat transfer for the microchannel with pin-fin at the bottom is the developing flow type conditions created by the fins on the flowfield. A periodically developing flow occurs in stream-wise direction of the channel and a completely fully developed condition never could be reached in the microchannel. This point was illustrated in figure 4 which shows the velocity component of the flow along x direction passing through nearly at the middle of the channel height and one-third of the channel width for a simple and a pin-finned microchannel. These higher velocities lead to a higher velocity gradient and enhance heat transfer on the wet surfaces of the microchannel.

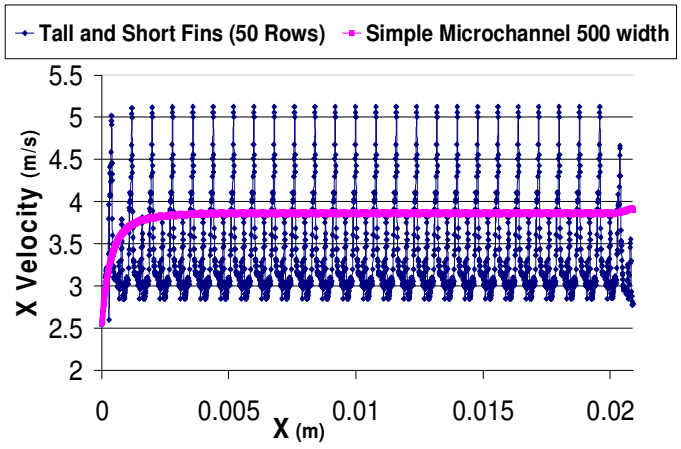

Figure 4. Comparison between the simple and pin-finned microchannels for X Velocity in the specified stream-wise direction of the microchannel at Re= 387.

Also when micro pin-fins were used in channels, higher temperatures were achieved. Figure 5 shows the temperature distribution along the stream-wise direction for both simple and pin-finned microchannels. As this figure shows the fluid temperature increases with a much higher rate for the pin-finned microchannel due to a higher heat transfer coefficient and effective area. Flow reaches to a thermally fully developed condition close to the end of the pin-finned microchannel length.

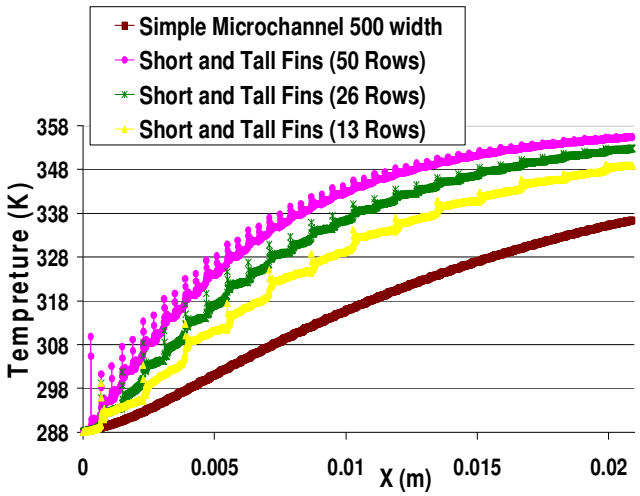

Figure 5. Comparison between the simple and pin-finned microchannels for static temperature in the specified stream-wise direction of the channel, Re= 387, Tin=15° C, T_s= 85° C.

No heat transfer enhancement would be complete without an investigation of the pressure drop in the microchannel. As figure 6 illustrates, this heat transfer enhancement will come at the price of added pressure drop and friction factor. The friction factor is defined as:

$$f = \frac{\Delta P}{4(l/D_h)(1/2)\rho_f U_{in}^2} \qquad (5)$$

The friction factor for pin-finned microchannel is much higher as compared with a simple microchannel. The fabricated fins on the bottom surfaces of the microchannels have a major effect on the increase of pressure drop in the microchannel. The enhancement heat transfer should be carefully weighed with the added pressure penalty. It is critical to measure the overall pressure drop in order to properly size a fluid pump. The pin-fins heights and also the row distances have a major effect in the pressure drop. As the figure 6 shows the case in which all tall fins fitted with channel height has the highest pressure drop. Decrease of the fins height and also increase of the row distances lowers the pressure drop considerably. So the lowest pressure drop among all pin-finned cases belongs to the case with 13 rows of short fins. This trend can be justified easily because with a short fin and also higher fins distance the friction drag would be smaller as a result of lower wetted surface in the channel. Recalling the acceptable limit of the heat transfer removal for highly distant and short fins cases, their low pressure drop makes them attractive for the purpose of heat transfer enhancements.

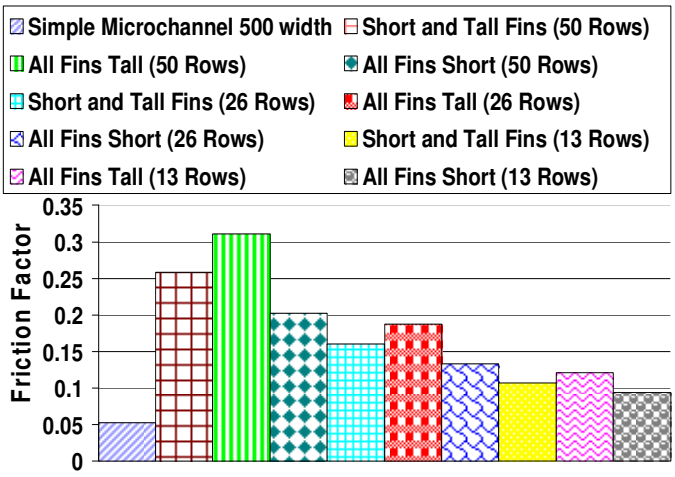

Figure 6. Comparison of friction factor for the simple microchannel and microchannels with different scheme of cylinders, T_s= 85° C, Re= 387.

To compare properly the different microchannel heat exchanger geometries, a parameter including both dissipated heat flux and the pressure drop should be introduced. Therefore, a parameter called the pumping power flux developed by Steinke and Kandlikar [6] was used in the present study for the comparison of pin-finned microchannels.
This pumping power parameter was defined as follows:

$$P = \frac{\dot{m}\Delta p}{\rho} \qquad (6)$$

Dividing by the free flow area, the pumping power can be manipulated to a flux term. Equation (7) shows the formula for the pumping power flux, or the pumping flux

$$P'' = \frac{\dot{m}\Delta p}{\rho A_{free}} \qquad (7)$$

where A_{free} is the free flow area. The heat and pumping power fluxes can be related in a simple manner in a coefficient of performance COP.
For the present work, the COP will be the desired dissipated heat flux divided by the required pumping power flux

$$COP = \frac{q''}{p''} \qquad (8)$$

Substituting Eq.(7) in Eq.(8) leads to

$$COP = \frac{\rho q''}{\dot{m}\Delta p} A_{free} \qquad (9)$$

Figure 7 compares the COP of a simple microchannel and the discussed pin-finned microchannels. As this figure shows the simple microchannel has a higher COP compared with microchannels with cylindrical microstructures. This is because of very high pressure drop of finned microchannels. The highest COP for microchannels with fabricated cylindrical fins corresponds to the case with 13 rows of the short cylinders; this case has also the lowest pressure drop. In fact, the effect of increased wetted area on the pressure drop is more noticeable compared with enhancing the heat transfer for cylindrical microstructures. Abouali and Baghernezhad [17] showed that fabrication of the grooves on the floor and side walls of a microchannel increases both the heat removal and COP. So using grooved microchannels is preferable compared with pin-finned microchannels especially for less pressure drop criteria.

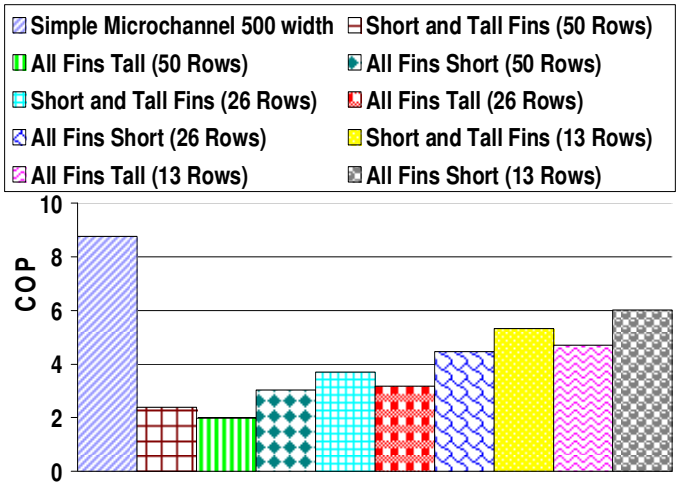

Figure 7. Comparison of COP for simple and micro pin-finned microchannels at Re= 387, T_s= 85° C.

In figure 8, the contours of velocity magnitude in the middle horizontal plane for the micro pin-finned microchannel are presented. The higher velocity near the fin passages can be seen in the figure. The velocity at the inlet of the microchannel is 2.55 m/s which increases to 5.9 m/s around the fins inside the microchannel. Velocities around tall fins are more than that for short ones, because of lower cross sectional areas.

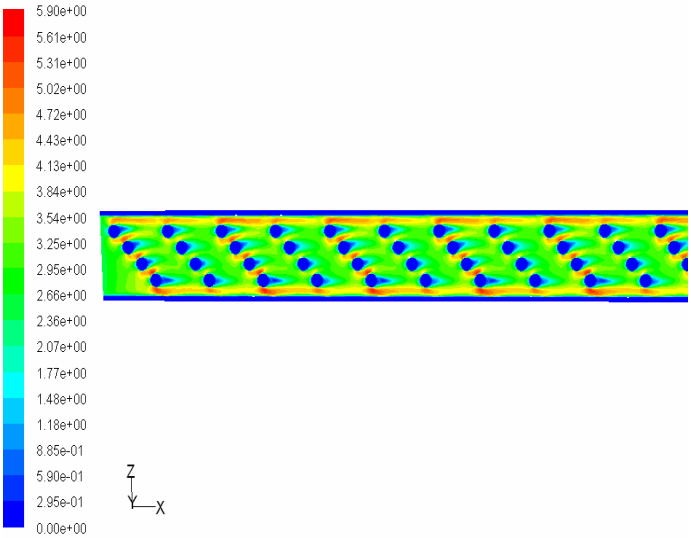

Figure 8. Velocity magnitude contours distribution in the middle horizontal plane of microchannel with micro pin-finned structures (Tall and Short fins-50 Rows). Re= 387, T_s= 85° C.

Figure 9 illustrates, velocity vectors colored by stream-wise velocity value at the same plane of figure 8 around some pin-fins. The minus sign of the stream-wise velocity magnitude shows the location of the reversed flows zones behind the

cylindrical micro fins.

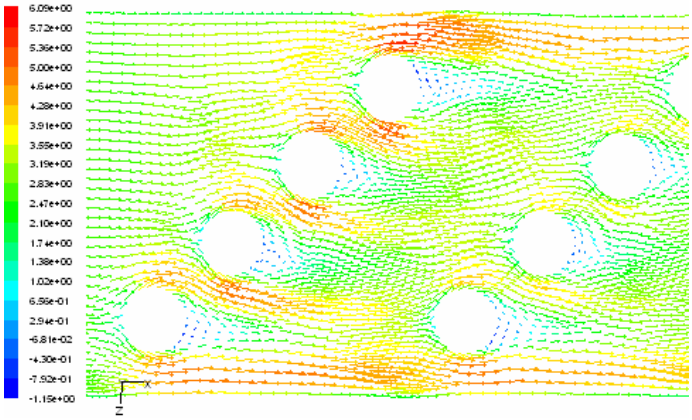

Figure 9. Velocity vectors in the middle horizontal plane of microchannel for micro pin-finned structures (Tall and Short fins-50 Rows) at Re= 387, T_s= 85° C.

One of the major simplifications in the present work is the steady flow assumption for the flow field that needs to be verified.

CONCLUSIONS

In this paper, the effects of nine types of various size and configurations of the cylindrical micro pin-fins on the heat transfer and friction factor of microchannels are investigated numerically. These cases include tall fins fitted in the channel height and short fins with a height equal to two-third of the channel height. Also three different distances of fin rows are examined.

In all cases, the cylindrical micro fins on the bottom of microchannel increases the heat removal flux but this includes the penalty of a much higher pressure drop and friction factor. The heat removal and pressure drop increase 22 percent and 83 percent, respectively in a pin-finned microchannel for a case with the tallest and highest numbers of the fins. With a decrease of the fin heights and also an increase of the distance between fins rows, the heat removal decreases not considerably but the decrease of pressure drop is much more noticeable.

As a final point, the coefficient of performance (which includes both the heat removal and pressure drop) of the studied pin-finned microchannels is lower compared with simple microchannels. So these types of microchannels are preferred when only the heat removal is of more concern.

REFERENCES

[1] Shah, R. K. and London, A. L., Laminar Flow Forced Convection in Ducts, Supplement 1 to Advances in Heat Transfer, New York: Academic Press, 1978.

[2] Kakac, S., Shah, R. K., and Aung, W., Handbook of Single-Phase Convective Heat Transfer, New York: John Wiley and Sons, Inc., 1987.

[3] Kishimoto, T. and Sasaki, S., Cooling characteristics of diamond-shaped interrupted cooling fins for high power LSI devices, Electron. Letter., 23(9), 456–457, 1987.

[4] Morini,G.L., Single-phase convective heat transfer in microchannels: a review of experimental results, Int. J. Therm. Sci. 43 (2004) 631–651.

[5] Kandlikar, S. G. and Grande, W. J., Evaluation of single-phase flow in microchannels for high flux chip cooling – thermo-hydraulic performance enhancement and fabrication technology, Heat Trans. Eng., 25(8), 5–16, 2004.

[6] Steinke, M. E. and Kandlikar, S. G., Single-phase enhancement techniques in microchannel flows, Paper No. ICMM2004-2328, ASME, Second International Conference on Microchannels and Mini-channels, Rochester, NY, June 17–19, 2004.

[7] Steinke, M. E., Characterization of single-phase fluid flow and heat transfer in plain and enhanced silicon microchannels, PhD Thesis, Rochester, NY: Microsystems Engineering, Rochester Institute of Technology, 2005.

[8] Kandlikar, S. G. and Upadhye, H. R., Extending the heat flux limit with enhanced microchannels in direct single-phase cooling of computer chips, Invited Paper presented at IEEE-Semi-Therm 21, San Jose, March 15–17, 2005.

[9] Colgan, E. G., Furman, B., Gaynes, M., Graham, W., LaBianca, N., Magerlein, J. H., Polastre, R. J., Rothwell, M. B., Bezama, R. J., Choudhary, R., Martson, K., Toy, H., Wakil, J., Zitz, J., and Schmidt, R., A practical implementation of silicon microchannel coolers for high power chips, Invited Paper presented at IEEE-Semi-Therm 21, San Jose, March 15–17, 2005.

[10] Tao, W. Q., He, Y. L., Wang, Q. W., Qu, Z. G., and Song, F. Q., 2002, "A Unified Analysis on Enhancing Single Phase Convective Heat Transfer With Field Synergy Principle," Int. J. Heat Mass Transfer, 45(24), pp. 4871–4879.

[11] Croce, G., Dàgaro, P. and Nonino, C., Three-dimensional roughness effect on microchannel heat transfer and pressure drop, Int. J. Heat Mass Transfer 50 (2007) 5249-5259.

[12] Cheng, Y.J., Numerical simulation of stacked microchannel heat sink with mixing-enhanced passive structure, International Communications in Heat and Mass Transfer 34 (2007) 295 –303.

[13] Zhong, X., Fan, Y., Liu, J., Zhang, Y., Wang, T. and Cheng, Z., A Study of CFD Simulation for On-Chip Cooling with 2D CNT Micro-fin Array, High Density packaging and Micro-system Integration 2007 HDP'07 International symposium on 26-28 June 2007.

[14] Hasan, M. I., Rageb, A.A., Yaghoubi, M. and Homayoni, H., Influence of channel geometry on the performance of a counter flow Microchannel heat exchanger, Int. J. Thermal Sciences 48 (2009) 1607–1618.

[15] Hong, F. and Cheng, P., Three dimensional numerical analyses and optimization of offset strip-fin microchannel heat sinks, Int. J. Heat Mass Transfer 36 (2009) 651–656.

[16] Kosar, A., Effect of substrate thickness and material on heat transfer in microchannel heat sinks, Int. J. of Thermal Sciences 49 (2010) 635-642

[17] Abouali, O. and Baghernezhad, N., "Numerical Investigation of Heat Transfer Enhancement in a Microchannel With Grooved Surfaces", Journal of Heat Transfer, Vol. 132, (4), 2010.